Supporting Information

Inverse opal manganese-doped Tungsten trioxide as a high-performance Fenton-like photocatalyst for levofloxacin degradation

Nan Jia[a,b], Yizhou Wu[a,b], Xinxi Zhang[a,b], Liang Zhou[a,b,c,d], Juying Lei[a,b,c,d,*], Tan Phong Nguyen[e], Jinlong Zhang[d,f], Yongdi Liu[a,b,d,*]

[a] *National Engineering Research Center of Industrial Wastewater Detoxication and Resource Recovery, East China University of Science and Technology, 130 Meilong Road, Shanghai 200237, P. R. China. Email: leijuying@ecust.edu.cn*

[b] *State Environmental Protection Key Laboratory of Environmental Risk Assessment and Control on Chemical Process, East China University of Science and Technology, 130 Meilong Road, Shanghai 200237, P. R. China. Email: ydliu@ecust.edu.cn*

[c] *Shanghai Institute of Pollution Control and Ecological Security, Shanghai200092, P.R. China*

[d] *Shanghai Engineering Research Center for Multi-media Environmental Catalysis and Resource Utilization, East China University of Science and Technology, 130 Meilong Road, Shanghai 200237, P. R. China*

[e] *Faculty of Biology and Environment, Ho Chi Minh City University of Industry and Trade (HUIT), 140 Le Trong Tan Street, Tay Thanh Ward, Tan Phu District, Ho Chi Minh City,70000,Vietnam*

[f] *Key Laboratory for Advanced Materials and Joint International Research Laboratory of Precision Chemistry and Molecular Engineering, Feringa Nobel Prize Scientist Joint Research Center, School of Chemistry and Molecular Engineering, East China University of Science and Technology, 130 Meilong Road, Shanghai 200237, P. R. China*

1. Tables

Table S1. Reagents.

Name	Molecular formula /abbreviation	Purities	Manufacturer
Anhydrous ethanol	C_2H_6O	AR	Aladdin
Sodium dodecyl sulphate	$C_{12}H_{25}O_4NaS$	GC	Macklin
Potassium persulfate	$K_2S_2O_8$	AR	Macklin
Styrene	C_8H_8	AR	Macklin
Methanol	CH_4O	AR	Aladdin
Ammonium metatungstate	$(NH_4)_6H_2W_{12}O_{40}.xH_2O$	AR	Macklin
Manganese chloride tetrahydrate	$MnCl_2 \cdot 4H_2O$	AR	Rhawn
Levofloxacin	$C_{18}H_{20}FN_3O_4$/LVX	AR	Adamas
Norfloxacin	$C_{16}H_{18}FN_3O_3$/NOR	AR	Macklin
Sulfadiazine	$C_{10}H_{10}N_4O_2S$	AR	Rhawn
Tetracycline	$C_{22}H_{24}N_2O_8$/TCH	AR	Macklin
Sodium thiosulfate	$Na_2S_2O_3$	AR	Macklin
Monopersulfate (potassium persulfate)	$K_2O_8S_2$/PMS	AR	Alfa-Aesar
2,2,6,6-Tetramethylpiperidine	$C_9H_{19}N$/TEMP	GC	Aladdin
p-Benzoquinone	$C_6H_4O_2$/BQ	AR	J&KScientific
Tertiary Butyl Alcohol	$C_4H_{10}O$/TBA	AR	Lingfeng, Shanghai
Sodium iodate	$NaIO_3$	AR	Adamas
Triethanolamine	$C_6H_{15}NO_3$/TEOA	GC	Rhawn
5,5-Dimethyl-1-pyrroline-N-oxide	$C_6H_{11}NO$/DMPO	AR	J&KScientific
Furfuryl alcohol	$C_5H_6O_2$/FFA	AR	Aladdin

Table S2. Equipments.

Name	Type	Manufacturer
Analytical balances	ME104E	METTLER TOLEDO
Ultra-pure water machine	OKP-S010 standard	Laike, Shanghai
Nitrogen Cylinder	/	Shenzhong, Shanghai
Vacuum Pump	SHZ-D(III), circulating water	Jinfu, Shanghai
Ultrasonic cleaner	SK3200H	Kedao, Shanghai
Magnetic Stirrer	ZM-85-1	Zhiwei, Shanghai
Temperature-controlled heating magnetic stirrer	ZNCL-GS	Daojing, Shanghai
Electrothermal constant temperature blast drying oven	DHG-9070A	Hualian, Shanghai
Xenon lamp	HXF300/300W	Jinyuan, Beijing
Liquid chromatography	SPD-M20A	SHIMADZU
Muffle Furnace	KSL-1200X	Kejin,Hefei

2. Texts

Text S1. Characterization tools

The crystalline phase is determined by powder X-ray diffractometry (XRD), and the 2θ values are determined between 5° and 80° using a Rigaku Ultima IV diffractometer with Cu-Ka radiation (λ = 1.5406 Å).

The specific surface area Brunauer-Emmett-Teller (BET) is measured by N_2 adsorption using a fully automated surface micropore and physical adsorption meter (ASAP2020) at 77 K.

Scanning electron microscope (SEM) images of the catalysts are taken using a JEOL JSM 6360 LV microscope from Nippon Electronics Corporation. Low-resolution (TEM) and high-resolution (HRTEM) transmission electron microscope images of the catalysts are taken using a Nippon Electron JEM 1400 and a JEOL JEM 2100 microscope, respectively.

The leaching content of metal ions (Mn and W) are determined using ICP-AES. The leaching content of metal ions is tested by a 15 mL solutions after a normal degradation experiment, filtered by a 0.22-micron Teflon syringe filter. After filtering the catalyst, 40 µL of $Na_2S_2O_3$ (250 mM) was added to the sample to terminate the reaction. Then we sent the sample to the school test center to measure the leaching concentration of specific elements. Inductively Coupled Plasma Atomic Emission Spectrometer (ICP-AES) analyzes under the following conditions: the instrument model is 167nm-785nm/725 purchased by America Agilent company. Analysis wavelength: 177nm-785nm; Optical resolution: 0.009nm (at 200nm); Grating line: 97.4L/mm, focal length: 400mm; Detection limit of typical elements (As, Cd, Cu, Zn): < 0.01mg/L.

The intensity signals of free radicals are determined by an electron paramagnetic resonance spectrometer (ESR). A Bruker model 100G-18KG/EMX-8/2.7 spectrometer is used for the determination with the following parameters: X-band microwave

bridge (X-band microwave bridge) at 9.3-9.9 GHz, L-band microwave bridge (L-band microwave bridge) at 30-400 KHz, X-band resonant cavity (X-band resonator) at 30-400 KHz, and X-band resonator (X-band resonator) at 30-400 KHz. band resonator (X-band resonator), and L-band resonator (L-band resonator).

X-ray photoelectron spectroscopy (XPS) of the catalysts is performed using a Perkin-Elmer PHI 5000C ESCA spectrometer to determine the chemical composition of the samples and the valence changes of the elements, in which the binding energy uses a C1s level of 284.8 eV as an internal standard.

The photoluminescence (PL) emission spectra of the catalysts are measured using Cary Eclipse at room temperature (25°C) through an excitation light of 400 nm.

The UV-Vis diffuse reflectance spectra (UV-Vis DRS) of the catalysts are measured using a Shimadzu UV-2600 spectrometer equipped with an integrating sphere assembly and using $BaSO_4$ as the reflectance sample.

The transient photocurrent response of the catalyst is carried out at room temperature using an electrochemical analyzer (Zahner, Zennium) on an electrochemical workstation with a standard three-electrode system. The working electrode is prepared by dispersing 5 mg of the sample in ethanol solution, sonicating it and taking 20 μL drops on the electrode and leaving it to dry. Samples are tested under visible light irradiation conditions (300 W xenon lamp) with 0.5 M Na_2SO_4 solution as electrolyte using the prepared samples as working electrode (active area of about 0.5 cm-2), platinum wire as counter electrode and saturated Hg/Hg_2Cl_2 as reference electrode.

Electrochemical impedance (EIS) is also measured on electrochemical workstation with a working electrode for samples (prepared as above), a platinum wire as counter electrode, and a saturated Hg/Hg_2Cl_2 as a reference electrode. A mixed aqueous solution of 0.025 M $K_3[Fe(CN)_6]$, 0.025 M $K_4[Fe(CN)_6]$, and 0.1 M KCl is used as the electrolyte.

Mott-Schottky measurements are also carried out on electrochemical workstation, and the reactive electrolytic cell is covered with a cardboard box to test different samples using a 0.5 M Na_2SO_4 solution as the electrolyte.

High-performance liquid chromatography (HPLC) analyzes under the following conditions: a 0.2% (v/v) aqueous formic acid solution and acetonitrile as mobile phase A and B, methanol and water as rinse solution, at a flow rate of 1.0 mL/min, and an injection volume of 20 μL. The instrument model is LC-2030C 3D Plus (SHIMADZU) and the UPLC column is a Shim-pack GIST C18 Column (2.1×100mm) from SHIMADZU at a column temperature of 302 K (30°C). The wavelengths of detection for levofloxacin, norfloxacin, sulphadoxine-pyrimethamine and tetracycline are 294 nm, 278 nm, 264 nm, and 355 nm, respectively.

Degradation products by ultra-performance liquid chromatography-tandem mass spectrometry (LC–MS/MS) analyzes under the following conditions: Molecular weight range 50-6000, resolution up to 140000. The instrument model is Q-Exactive plus. The ion source contains ESI ion source, APCI ion source and nanoESI ion source. The mass analyser adopts the combination of quadrupole and electrostatic field orbit trap in series. The liquid phase system is equipped with dual systems of ultra-high

pressure liquid chromatography and nanoliter liquid chromatography. The secondary mass spectrometry fragmentation mode (MS/MS): HCD. The data system (Software) used Xcalibur data acquisition system, MASS FRONTIER structure analysis software, COMPND DISC metabolomics software, PROTEOME DISCOVERER proteomics software, TRACEFINDER quantification software, and BIOPHARMA molecular weight deconvolution software, etc. Mass range 50-6000m/z; Instrument resolution: 140,000 FWHM (m/z≤200), ≥4 levels adjustable; High-resolution mass spectrometry acquisition rate: up to 12Hz; Mass axis stability: after the equipment calibrates once, the mass axis will not be corrected within 48 consecutive hours, and the mass accuracy is ≤2ppm; Sensitivity: Full Scan (m/z.) 100-900) Sensitivity (resolution≥70000 FWHM): 50fg reserpine injection, S/N>500:1, selective ion scanning SIM sensitivity (resolution≥70000 FWHM): 50fg reserpine injection S/N>1000:1, MS/MS sensitivity (resolution≥70000 FWHM): 50fg reserpine injection, S/N >1000:1.

Text S2. Quenching experiments

0.8142 mL of methanol (400 mM), 1.9518 mL of tert-butanol (400 mM), 1.764 mL of furfuryl alcohol (400 mM), 10.8 mg of p-benzoquinone (2 mM), 19.8 mg of $NaIO_3$ (2 mM), and 2.6546 mL of triethanolamine (400 mM) are added prior to the start of the reaction to quench $SO_4^{\bullet-}$ and $\bullet OH$, $\bullet OH$, $^1O_2$, $\bullet O_2^-$, e- and h^+.

Determination of the electron paramagnetic resonance (ESR) signals of $SO_4^{\bullet-}$, $^1O_2$, $\bullet O_2^-$ and $\bullet OH$ need to be carried out in a separate system as follows:

5 mg of catalyst powder and 50 μL of TEMP are added to 5 mL of aqueous solution. 40 μL of PMS (0.05 mol/L) and light are added after 1 min, and the solution

is filtered and injected into a capillary tube after 3 min to measure the ESR signals of $^1O_2$. Another set of PMS only without catalyst is measured as a control.

5 mg of catalyst powder and 50 μL of DMPO are added to 5 mL of methanol solution. 40 μL of PMS (0.05 mol/L) and light are added after 1 min, and the solution is filtered and injected into a capillary tube after 3 min to measure the ESR signals of $•O_2^-$. Another set of PMS only without catalyst is measured as a control.

5 mg of catalyst powder and 50 μL of DMPO are added to 5 mL of aqueous solution. 40 μL of PMS (0.05 mol/L) and light are added after 1 min, and the solution is filtered and injected into a capillary tube after 3 min to measure the ESR signals of $SO_4^{•-}$ and $•OH$. Another set of PMS only without catalyst is measured as a control.

3. Figures
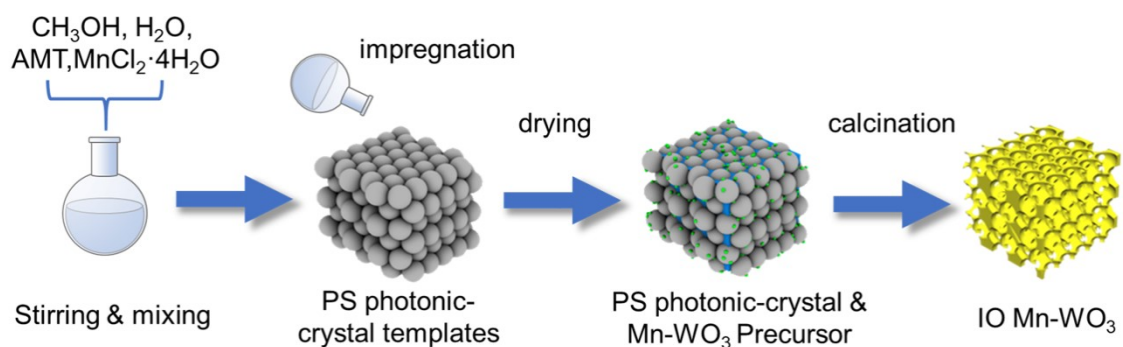
Fig. S1. The process of catalyst preparation.
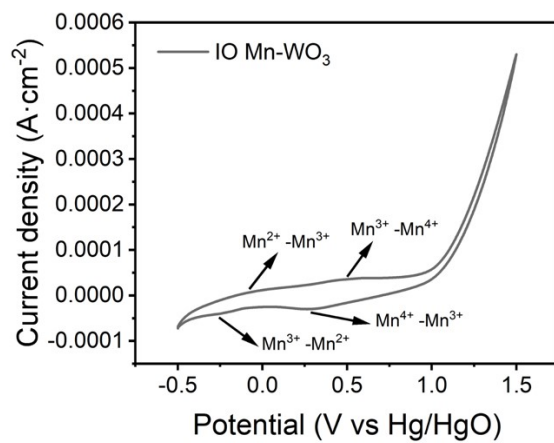
Fig. S2. CV curve of IO Mn-WO$_3$.
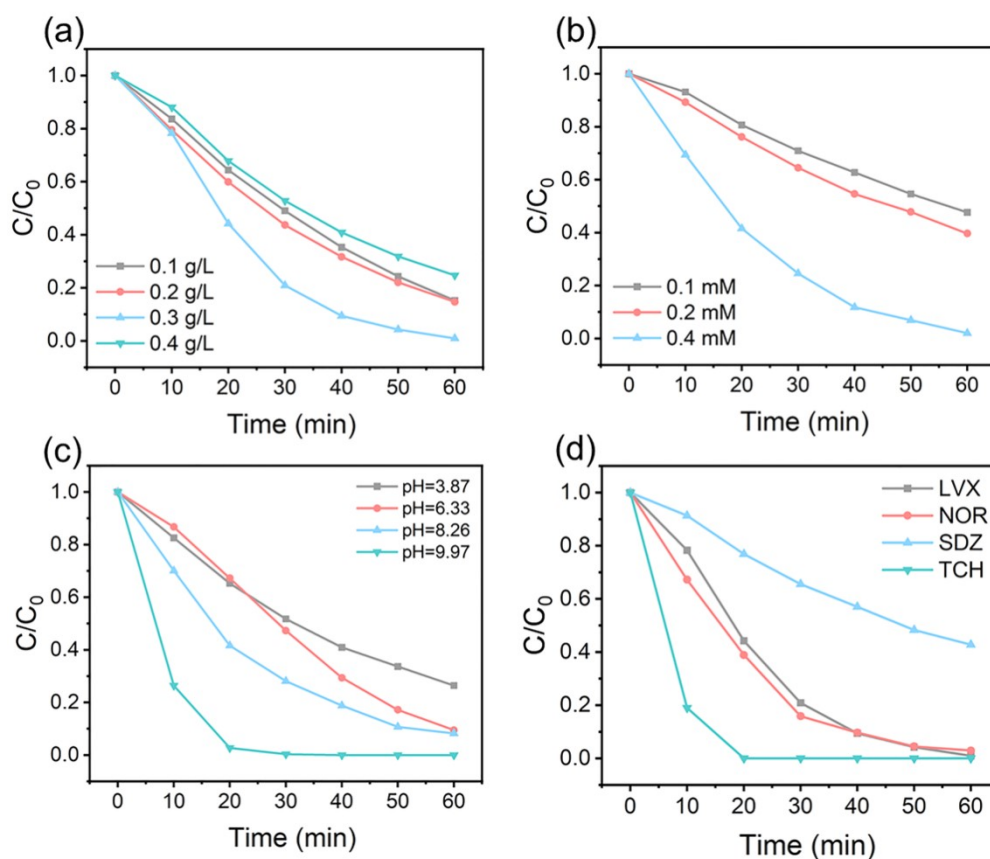
Fig. S3. The influence of different factors on the LVX degradation efficiency: (a) catalyst dosage; (b) PMS concentration; (c) pH; (d) different antibiotics. Reaction conditions: [Catalysts] = 0.3 g/L, [PMS]$_0$ = 0.4 mM, [LVX]$_0$ = 20 mg/L, with visible light irradiation.
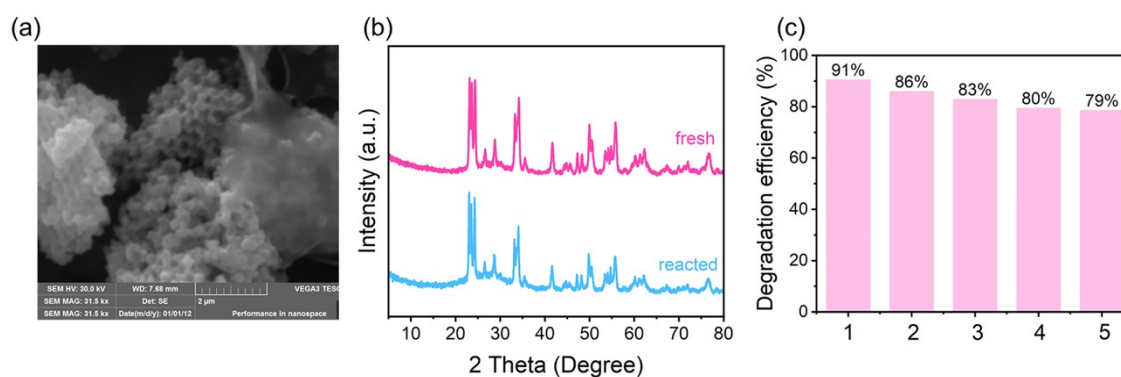

Fig. S4. (a) SEM image of the catalyst after the reaction; (b) XRD patterns of the catalyst before and after the reaction; (c) cycling tests. Reaction conditions: [Catalysts] = 0.3 g/L, [PMS]$_0$ = 0.4 mM, [LVX]$_0$ = 20 mg/L, with visible light irradiation.
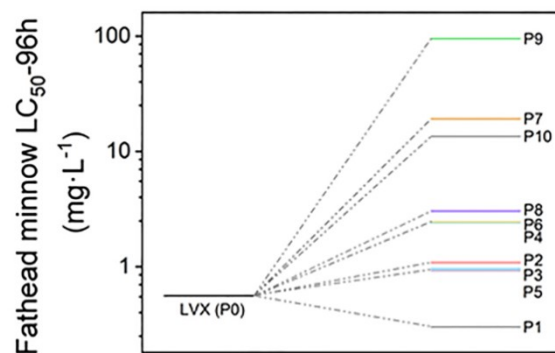
Fig. S5. Toxicity assessment of reaction intermediates (using fathead minnow LC_{50}-96h as an indicator).
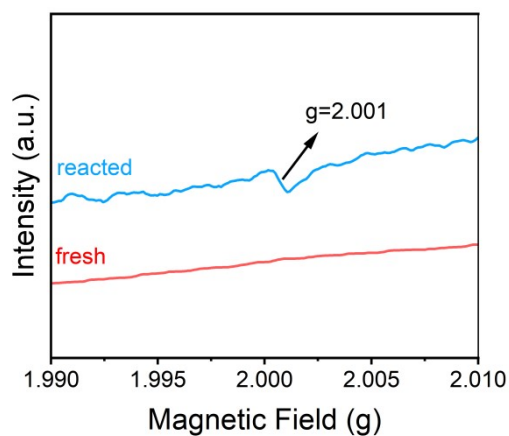
Fig. S6. Electron spin resonance (ESR) spectra of IO Mn-WO_3 before and after reactions.
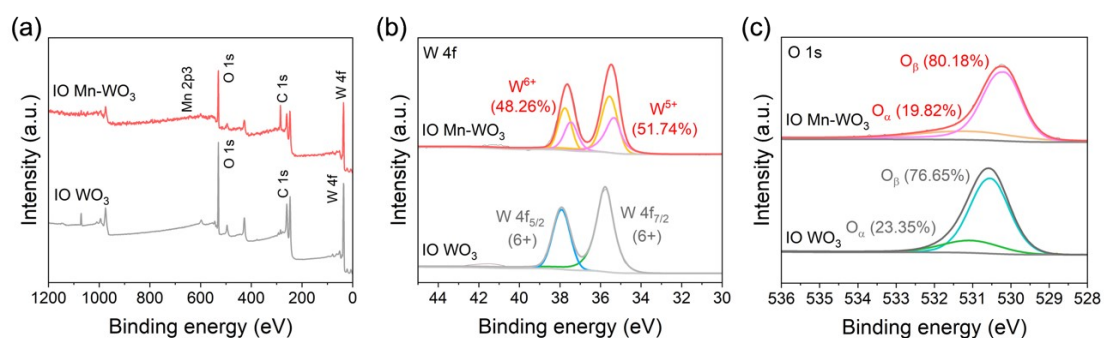

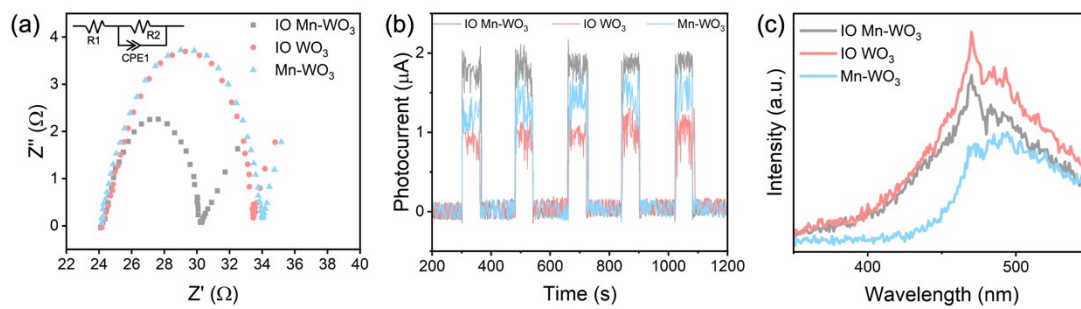**Fig. S7.** XPS spectra of IO Mn-WO_3 and IO WO_3. (a) full XPS survey; (b) W 4f; (c) O 1s.

Fig. S8. (a) EIS-Nyquist plots of different catalysts; (b) transient photocurrent response plots under visible light irradiation; (c) photoluminescence (PL) spectra (excitation wavelength at room temperature: 400 nm)
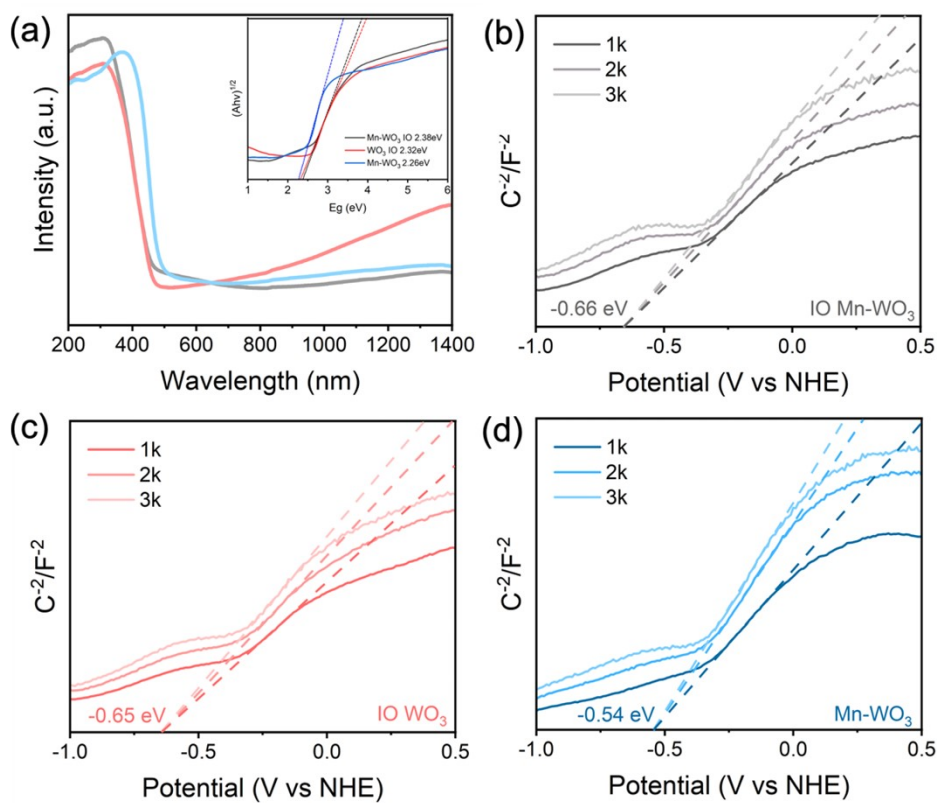

Fig. S9. (a) UV-visible diffuse reflectance spectra; (b-d) Mott-Schottky plots for different catalysts.
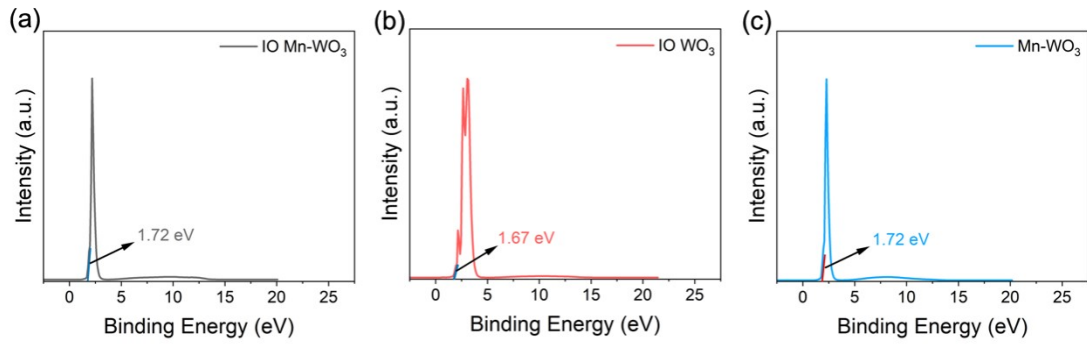
Fig. S10. Valence band XPS spectrum of (a) IO Mn-WO$_3$, (b) IO WO$_3$ and (c) Mn-WO$_3$.
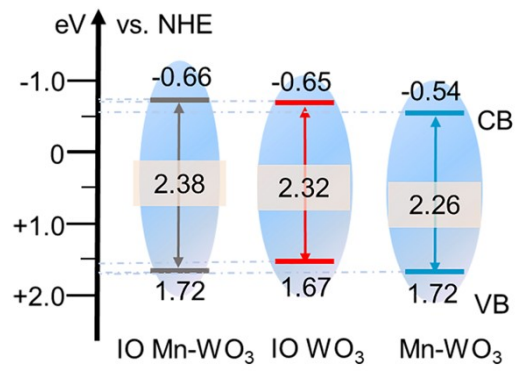

Fig. S11. Energy band structure of the three samples.

4. Tables

Table. S3. The electrochemical impedance spectroscopy (EIS) of IO Mn-WO_3, IO WO_3 and Mn-WO_3

	IO Mn-WO_3	IO WO_3	Mn-WO_3
R1/Ω	4.6	4.6	4.6
R2/Ω	6	9.5	10